VOL. 21, NO. 7, APRIL 2026 ISSN 1819-6608
ARPN Journal of Engineering and Applied Sciences

www.arpnjournals.com

PREDICTING OF NONLINEAR DEFLECTION OF BEAMS USING ARTIFICIAL NEURAL NETWORKS

Hanane Moulay Abdelali and Rhali Benamar
École Mohammadia d'Ingénieurs, Mohammed V University in Rabat, LERSIM, Avenue Ibn Sina B. P., Agdal, Rabat, Morocco
E-Mail: moulayabdelali@emi.ac.ma

ABSTRACT

In this paper, artificial neural networks (ANNs) are used to predict the nonlinear deflection of beams subjected to concentrated loads at different sections and under various limit boundaries. The research focuses on developing ANN models capable of accurately predicting large deflections of beams. A comprehensive dataset, generated through semi-analytical methods, finite element simulations, and experimental results, was used to train and validate the models. The input variables included excitation force, contribution coefficient, and linear and nonlinear terms of rigidity. The performance of the ANN models was evaluated by comparing predicted deflections with known data available in the literature, showing high accuracy and reliability. The results demonstrate the potential of ANN-based approaches for efficient and accurate deflection prediction in structural engineering applications, offering a valuable tool for designing and analyzing beams in complex loading scenarios.

Keywords: artificial intelligence, beam, deflection, statique, nonlinear, predictive modelling, ANN.

Manuscript Received 15 March 2026; Revised 2 April 2026; Published 10 June 2026

1. INTRODUCTION

Predicting how beams bend and deflect under various loads is a core challenge in structural engineering, especially when dealing with complex, nonlinear behaviors. Traditional analytical methods can be time-consuming and may struggle to capture the full picture, particularly as loads and deflections increase. In recent years, artificial neural networks (ANNs) have gained attention as powerful tools for predicting complex behaviors in engineering, particularly in structural analysis.

Murali Krishna *et al.*, 2020 include an experimental section that enabled plotting stress-strain curves from compression tests, using an image-based methodology to extract the data. It also includes a section on the validation of finite element results and the training of artificial neural networks (ANN). The experimental results, simulations, and predictions are in good agreement.

Song and Yu, 2013 studied the bending of a T-beam using the three-point bending method. The effect of material properties on springback is examined through numerical simulations using the finite element method, with results validated experimentally. The simulation data enabled the development of a neural network model for predicting springback.

Sakr and Sakla, 2009 used two approaches to study the short- and long-term deformations of supported composite beams: finite element analysis and artificial neural networks (ANN). The nonlinear load-slip relationship of the shear connectors was incorporated into the finite element model. Two ANN models were developed and trained using a very large database. These models allowed for predicting the deformations of composite beams with new properties and assessing the effects of geometric design variables on the short- and long-term deformations of simply supported composite beams. The results from the finite element model were used to estimate short- and long-term deformations, revealing that the AISC specifications underestimate short-term deformations and overestimate long-term deformations.

The inelastic deformation of clamped metal beams impacted by a mass was predicted by Hosseini and Abbas, 2012 based on an empirical relationship and a neural network model developed using independent variables such as material properties and the geometry of the impactor and the beam. The experimental results are in good agreement with the predicted maximum deformations for various impact energies.

In (Hoan and al. 2020), the deformation of reinforced concrete beams with fiber-reinforced polymer (FRP) bars was predicted by developing a genetic expression programming (GEP) model. The calculation of the effective moment of inertia for 108 beams created a database to train the GEP. The predicted results were verified using experimental data. An acceptable prediction of the effect of tensile stiffness was also achieved by the GEP model.

The aim of the authors (Hasançebi and Dumlupınar, 2013) is to update finite element (FE) models for reinforced concrete (RC) T-beam bridges by developing efficient methods based on artificial neural networks (ANN). The ANN was trained using data generated from linear and nonlinear analyses. A comparison was made between the results obtained from the calibrated FE models and field measurements to determine the accuracy of the estimated parameters and the success of the updated model. The study demonstrates the reliability of the model and highlights the need for such analysis. It also shows that ANNs can be effectively and reliably used for parameter estimation tasks under high levels of uncertainty and complexity arising from the aging and deterioration of RC bridges, as well as the nonlinear properties of concrete in the nonlinear response for RC bridge parameter identification.

In (Tadesse and al., 2012), the prediction of deformations under service load in steel-concrete composite bridges was carried out by developing three neural networks corresponding to simply supported bridges, two-span continuous bridges, and three-span continuous bridges. The finite element software ABAQUS was used to generate the training and testing data. The neural networks were validated for several bridges by estimating the errors, which were found to be low.

In this study, we explore the use of artificial neural networks (ANNs) to predict nonlinear beam deflections with high accuracy. By training these models on a large and diverse dataset that combines semi-analytical results, finite element simulations, and experimental data, we aim to create a reliable tool that can simplify this prediction process. The ANN models take into account critical variables, such as applied force, structural contribution factors, and both linear and nonlinear rigidity terms. When tested, the models showed excellent alignment with established data, proving their accuracy and reliability. This approach demonstrates how ANNs can enhance our ability to analyze and design beams under varying and complex loading conditions, offering a new pathway toward faster, more efficient structural design solutions.

2. ARTIFICIAL NEURAL NETWORKS (ANNS) MODELING

Artificial neural networks (ANNs) serve as versatile tools for modeling the relationships between multiple input (independent) variables and one or more output (dependent) variables when there are complex and non-linear relationships between them. This analysis can handle several variables simultaneously, allowing for the capture of more sophisticated interactions and multidimensional relationships within the data. ANNs are composed of interconnected neurons or nodes, each with assigned synaptic weights determining their influence. They represent a family of adaptive computational tools capable of capturing non-linear behaviors in complex problem domains.

Artificial neural networks (ANNs) receive input signals that are affected by corresponding multiplier coefficients, known as synaptic weights and biases, Figure-1. These resulting values are then summed together. This sum constitutes the total input for a particular neuron before being passed through an activation function, which serves to excite or activate the neurons. In other words, in a summation layer, the various contributions from the weighted signals are combined to produce an aggregate value that represents the total activity of the neuron before the next processing step.

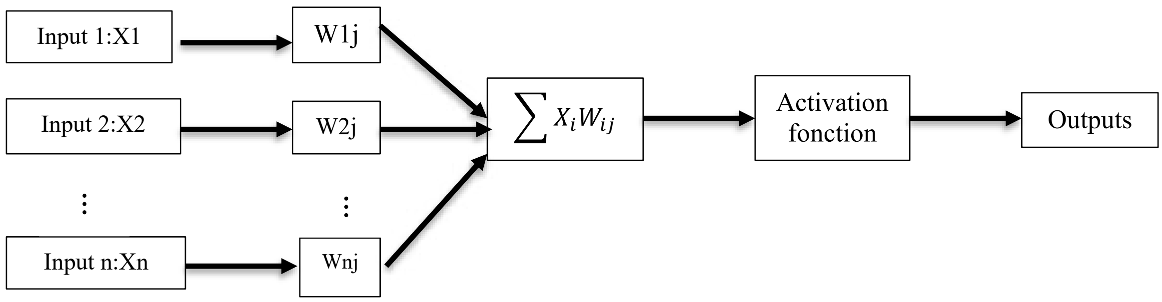

Figure-1. Structure of neural network.

The input vector [x1, x2, x3, ..., xk] is multiplied by the synaptic weights, which are then sent into a summation junction. The resulting sum is the dot product of the synaptic weight matrix and the input vector x. Additionally, the bias μ is incorporated into the summation layer. This combined sum is then passed through an activation function, which serves to excite or activate the neurons.

The synaptic weights are defined by the following matrix:

$$W = \begin{pmatrix} w_{11} & \cdots & w_{1n} \\ \vdots & \cdots & \vdots \\ w_{i1} & \cdots & w_{in} \end{pmatrix} \tag{1}$$

The mathematical expression for the output yi is given by the following equation:

$$y_i = f\left(\sum_n w_{in} x_n + \mu_i\right) \tag{2}$$

Where:

x_n: is the input impulse
w_{in}: are the synaptic weights
μ_i: are the biases
f: is the transfer function

One commonly employed transfer function is the sigmoid function, which adjusts output values within the range of 0 to 1, regardless of the input's initial range (which may span from negative to positive infinity).

Neural networks trained using the backpropagation algorithm are networks that utilize a supervised learning method. The backpropagation algorithm adjusts the weights of the connections between neurons by calculating the error between the network's predictions and the expected values. This error is then propagated backward through the network to adjust the weights to minimize the error. This process allows the network to gradually improve in the task it is assigned, such as predicting numerical values. The sigmoid function is particularly favored in these neural networks because it can be differentiated at any point in its domain.

Experimental and numerical results are validated through a judicious choice of an artificial neural network.

The Levenberg-Marquardt learning algorithm, which is selected for this study, begins with forward propagation, where the synaptic weights are multiplied by the input data and then propagated to the output layer through the hidden layers.

Next, the predicted values are compared to the actual values by calculating an error. If the error exceeds the acceptable limit, iterative adjustments of the synaptic weights at each neuron are made by initiating backpropagation within the neural network until the acceptable error is reached.

The neural network model for rectangular beams consists of an input layer with various variables, a hidden layer with 10 neurons, and an output layer with one output variable.

For the training phase, we considered 70% of the data. For testing, we allocated 15% of the data, and the remaining 15% was used for validation.

The preprocessing of the data is performed automatically. To minimize the absolute learning error as much as possible, the number of neurons in the hidden layers is determined iteratively.

The performance of the constructed network is evaluated using the correlation coefficient defined by equation (3), the mean absolute error (MAE) defined by equation (4), and the root mean square error (RMSE), defined by equation (5).

$$RMSE = \sqrt{\frac{1}{N}\sum_{i=1}^{N}(p_i - o_i)^2} \tag{3}$$

$$R = \frac{\sum_{i=1}^{N}(p_i - \bar{p})(o_i - \bar{o})}{\sqrt{\sum_{i=1}^{N}(p_i - \bar{p})^2(o_i - \bar{o})^2}} \tag{4}$$

$$\mathrm{MAE} = \frac{1}{\mathrm{N}}\sum_{\mathrm{i}=1}^{\mathrm{N}}(\mathrm{p_i} - \mathrm{o_i}) \tag{5}$$

The parametric study of artificial neural network (ANN) configurations with 10 neurons was deemed optimal. The calculated and predicted values of DI are Oi and Pi, where N is the number of validated samples. The average values of O¯ and P¯ represent the mean values of Oi and Pi, respectively.

We used the sigmoid activation function, as represented in Eq. (6), which is a very common choice for feed-forward neural networks. The network's output values are constrained between 0 and 1.

$$\emptyset_x = \frac{1}{1+e^{-x}} \tag{6}$$

3. PREDICTIVE MODELING USING ANNS

Simply supported and fixed-end steel beams are considered. The deflection is calculated theoretically and numerically using the Rayleigh-Ritz method (Moulay Abdelali and Benamar, 2024) at the center of the beam, as well as at one-quarter and three-quarters of its section.

We modeled a backpropagation artificial neural network and adopted the Levenberg-Marquardt algorithm (trainlm) to train it. The sigmoid function serves as the transfer function between the input layer and the hidden layer, while the purelin function represents the transfer function between the hidden layer and the output layer.

Four distinct neural networks are trained: two for the linear and nonlinear cases of simply supported beams, and the other two for the linear and nonlinear cases of fixed-end beams.

The predictions from the artificial neural networks (ANNs) are validated by comparing them with theoretical values and values found in the literature.

In the following of this article, the input variables used, defined in the reference (Moulay Abdelali and Benamar, 2024), are as follows:

F^*_1	is the dimensionless force applied to the beam;
a_i	is the contribution coefficient for i=1,…,n
Kij*	are the non-dimensional linear rigidity generalized parameters for i=1,…,n and j=1,…,n
b^*_{ijkl}	are non-dimensional non-linear rigidity generalized parameters for i=1,…,n ; j=1,…,n; k=1,…,n and l=1,…,n
W*max	is the non-dimensional deflection of the beam.

3.1 Prediction of the Static Linear Response at the Center of a Simply Supported Beam

For the linear case, the neural network consists of an input layer with 13 input variables, a hidden layer with 10 neurons, and an output layer with a single output variable.

The input vectors for the rectangular beams illustrated in Table-1 are the excitation F_1*, the beam functions: w_1*, w_3*, w_5*, w_7*, w_9*, w_{11}*, and the stiffness values: K_{11}*, K_{33}*, K_{55}*, K_{77}*, K_{99}*, K_{1111}*. The output vector is the maximum deflection (W_{max}*).

ARPN Journal of Engineering and Applied Sciences

www.arpnjournals.com

Table-1. The input vectors for the linear static response at the Center of a Simply Supported Beam.

F_1*	w_1*	w_3*	w_5*	w_7*	w_9*	w_{11}*	K_{11}*	K_{33}*	K_{55}*	K_{77}*	K_{99}*	K_{1111}*
[0-7.5]	1	-1	1	-1	1	-1	48,7	3945,1	30440,3	116939,6	319550,5	713083,2

The neural network diagram is shown in Figure-2 (a).

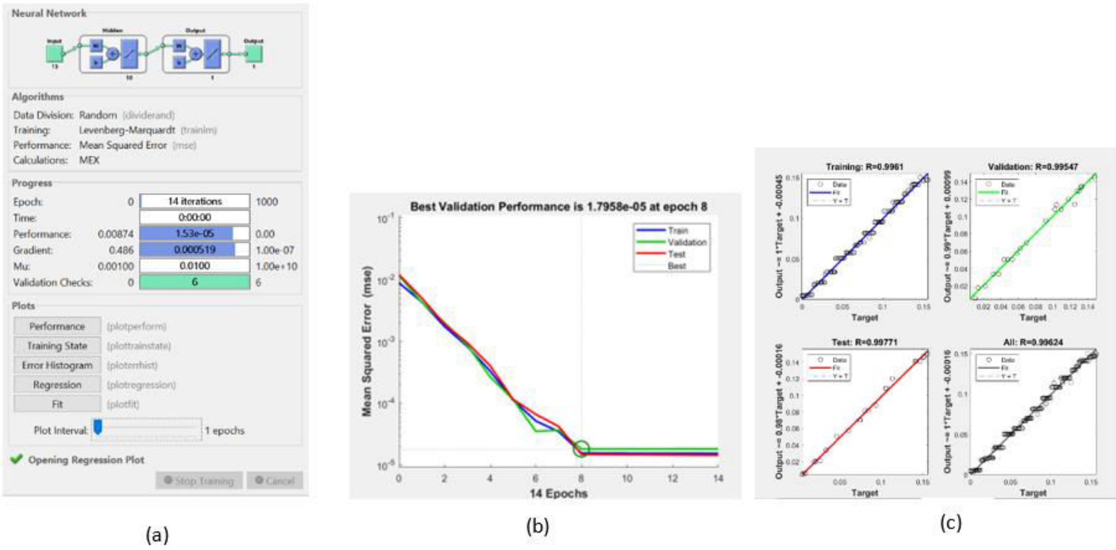

Figure-2. Schematic Representation of ANNs Architecture, Performance graph, and Regression graph for Rectangular Static Linear Response at the Center of a Simply Supported Beam.

According to Figure-2 (b), the neural network stops at the 14th epoch, and the mean squared error (MSE) at that point is close to 10^{-5}.

The value of R from the regression analysis is 0.9977, as shown in Figure-2 (c).

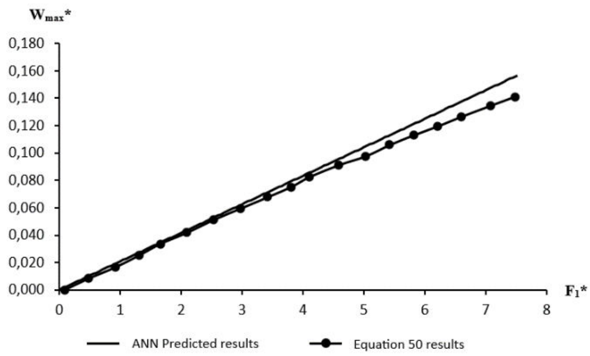

Figure-3. Comparison between the predicted results from the artificial neural network (ANN) and those from Equation 50 (Abolfathi and al. 2010).

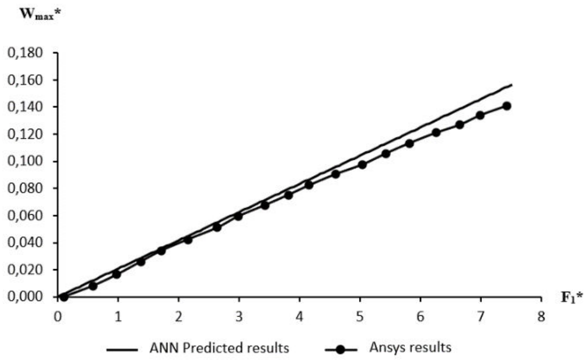

Figure-4. Comparison between the prediction results from the artificial neural network (ANN) and numerical result (Moulay Abdelali and Benamar, 2024).

3.2 Prediction of the Static Linear Response at One-Quarter and Three-Quarters of a Simply Supported Beam

For the linear case, the neural network consists of an input layer with 11 input variables, a hidden layer with 10 neurons, and an output layer with a single output variable. The input vectors for the rectangular beams illustrated in Table-2 are the excitation F_1*, the beam functions: w_1*, w_2*, w_3*, w_5*, w_6*, and the stiffness values: K_{11}*, K_{22}*, K_{33}*, K_{55}*, K_{66}*. The output vector is the maximum deflection (W_{max}*).

ARPN Journal of Engineering and Applied Sciences

Table-2. The input vectors for the linear static response at the One-Quarter and Three-Quarters of a Simply Supported Beam.

F_1*	w_1*	w_2*	w_3*	w_5*	w_6*	K_{11}*	K_{22}*	K_{33}*	K_{55}*	K_{66}*
[0-7.5]	0,71	1	0,71	-0,71	-1	48,70	779,27	3945,07	30440,34	63121,09

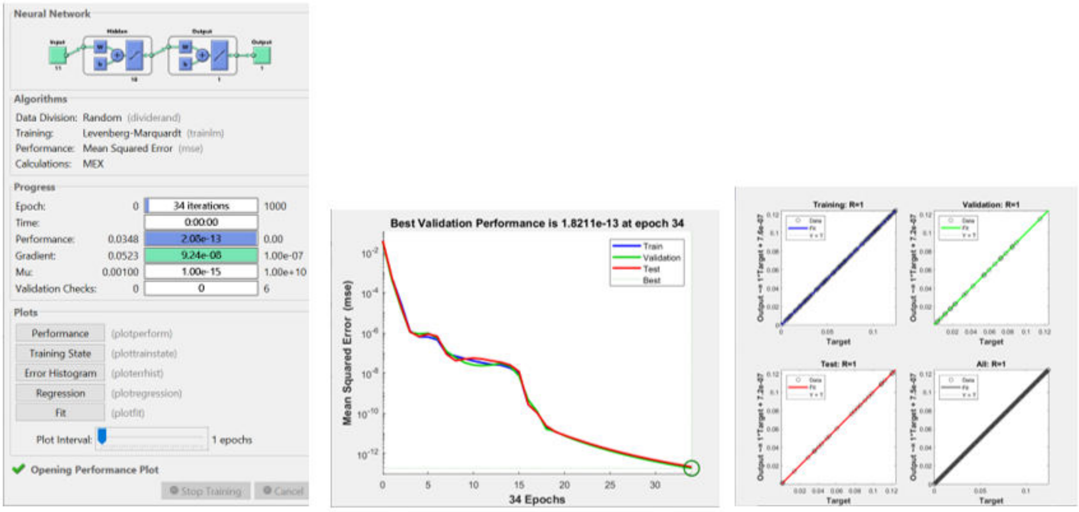

(a) (b) (c)

Figure-5. Schematic Representation of ANNs Architecture, Performance graph, and Regression graph for Rectangular Static Linear Response at the One-Quarter and Three-Quarters of a Simply Supported Beams.

The neural network diagram is shown in Figure-5 (a). According to Figure-5 (b), the neural network stops at the 34th epoch, and the mean squared error (MSE) at that point is close to 10^{-13}. The value of R from the regression analysis is 1, as shown in Figure-5 (c).

3.3 Prediction of the Static Nonlinear Response at the Center of a Simply Supported Beam

For the nonlinear case, the neural network consists of an input layer with 15 input variables, a hidden layer with 10 neurons, and an output layer with a single output variable.

The input vectors for the rectangular beams illustrated in Table-3 are the excitation F1*, the contribution coefficient is the contribution coefficient in the ith basic function used in the series expansion of transverse displacement a1, the beam functions: w_1*, w_3*, w_5*, w_7*, w_9*, w_{11}*, the stiffness values: K_{11}*, K_{33}*, K_{55}*, K_{77}*, K_{99}*, K_{1111}* and the nonlinear stiffness b_{1111}*. The output vector is the maximum deflection (W_{max}*).

Table-3. The input vectors for the nonlinear static response at the Center of a Simply Supported Beam.

F_1*	a_1	w_1*	w_3*	w_5*	w_7*	w_9*	w_{11}*	K_{11}*	K_{33}*	K_{55}*	K_{77}*	K_{99}*	K_{1111}*	b_{1111}*
[0-85]	[0-0.76]	1	-1	1	-1	1	-1	48,70	3,9 10^3	3,04 10^4	11,6 10^4	31,9 10^4	71,3 10^4	73,06

The neural network diagram is shown in Figure-6(a).

ARPN Journal of Engineering and Applied Sciences

www.arpnjournals.com

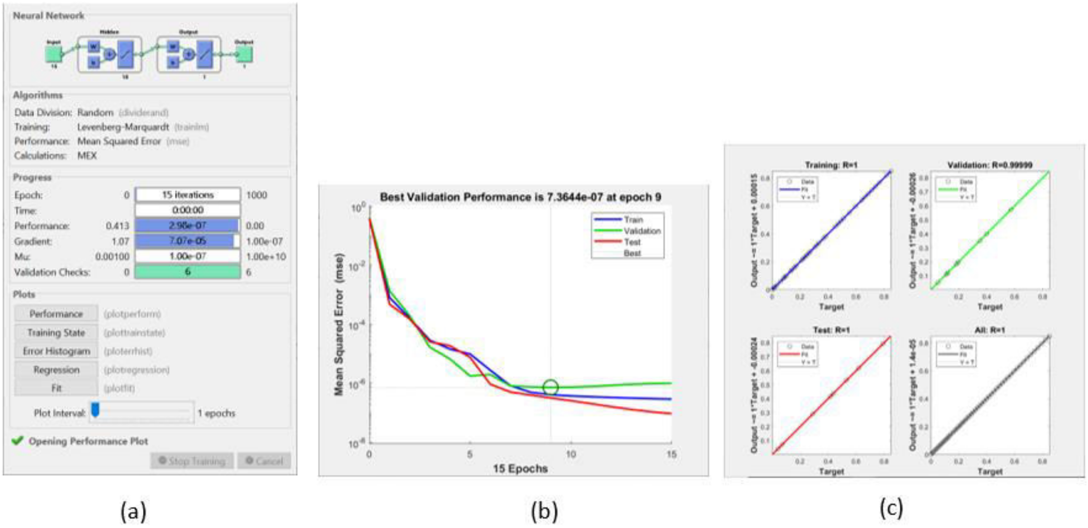

Figure-6. Schematic Representation of ANNs Architecture, Performance Graph, and Regression Graph for Rectangular Static Nonlinear Response at the Center of a Simply Supported Beam.

According to Figure-6 (b), the neural network stops at the 15th epoch, and the mean squared error (MSE) at that point is close to 10¯6. The value of R from the regression analysis is 1, as shown in Figure-6 (c).

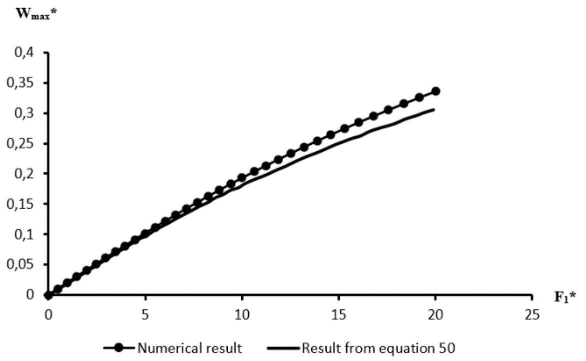

Figure-7. Validation of numerical results with the results of equation 50 (Abolfathi and al. 2010).

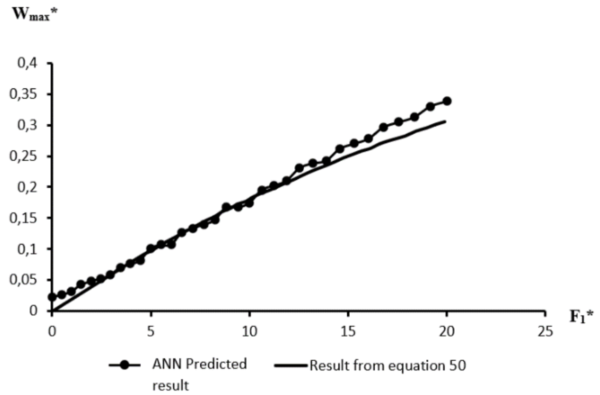

Figure-8. Validation of the results predicted by ANN with the results of equation 50 (Abolfathi and al. 2010).

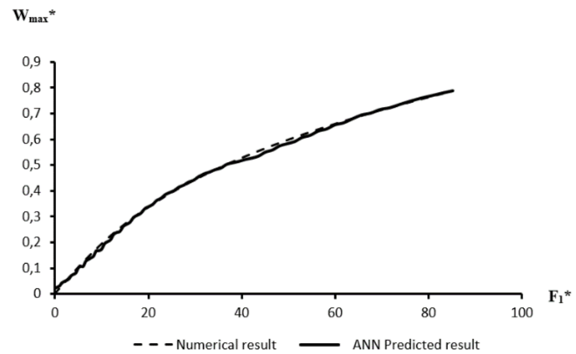

Figure-9. Validation of numerical results with the results predicted by ANN.

VOL. 21, NO. 7, APRIL 2026 ISSN 1819-6608
ARPN Journal of Engineering and Applied Sciences

3.4 Prediction of the Static Nonlinear Response at One-Quarter and Three-Quarters of a Simply Supported Beam

For the nonlinear case, the neural network consists of an input layer with 13 input variables, a hidden layer with 10 neurons, and an output layer with a single output variable.

The input vectors for the rectangular beams illustrated in Table-4 are the excitation F_1*, the contribution coefficient a_1, the beam functions: w_1*, w_2*, w_3*, w_5*, w_6*, the stiffness values: K_{11}*, K_{22}*, K_{33}*, K_{55}*, K_{66}* and the nonlinear stiffness b_{1111}*. The output vector is the maximum deflection (W_{max}*).

Table-4. The input vectors for the nonlinear static response at the One-Quarter and Three-Quarters of a Simply Supported Beam.

F^*_1	a_1	w_1*	w_2*	w_3*	w_5*	w_6*	K_{11}*	K_{22}*	K_{33}*	K_{55}*	K_{66}*	b^*_{1111}
0-40	0-0.52	0,71	1	0,71	-0,71	-1	48,7	779,3	3,9 10^3	30,4 10^3	63,1 10^3	73,05

The neural network diagram is shown in Figure-10(a).

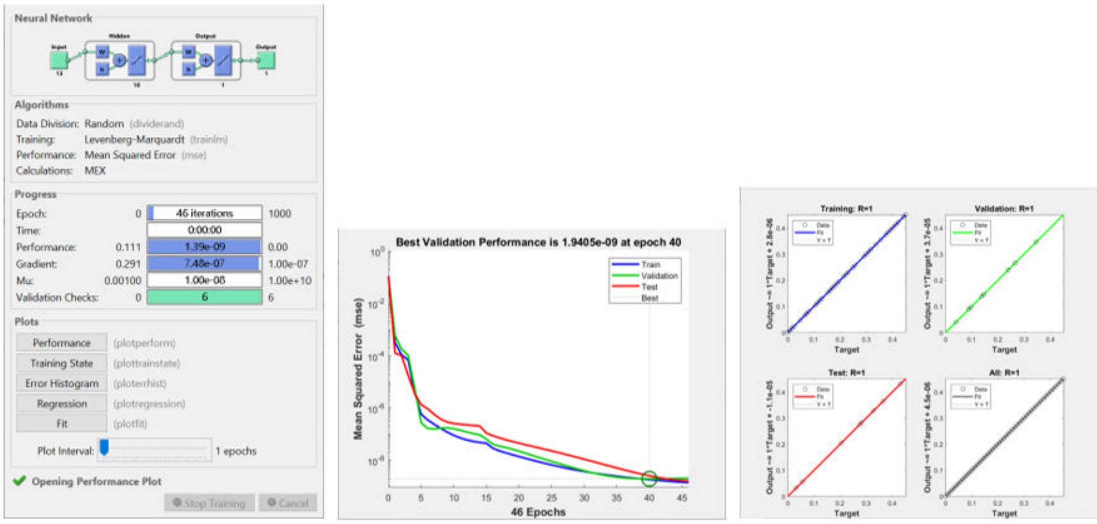

(a) (b) (c)

Figure-10. Schematic Representation of ANNs Architecture, Performance graph, and Regression graph for Rectangular Static Nonlinear Response at the One-Quarter and Three-Quarters of a Simply Supported Beams.

According to Figure-10 (b), the neural network stops at the 15th epoch, and the mean squared error (MSE) at that point is close to 10^{-9}. The value of R from the regression analysis is 1, as shown in Figure-10 (c).

3.5 Prediction of the Static Linear Response at the Center of a Clamped-Clamped Beam

For the linear case, the neural network consists of an input layer with 13 input variables, a hidden layer with 10 neurons, and an output layer with a single output variable.

The input vectors for the rectangular beams illustrated in Table-5 are the excitation F_1*, the beam functions: w_1*, w_3*, w_5*, w_7*, w_9*, w_{11}*, and the stiffness values: K_{11}*, K_{33}*, K_{55}*, K_{77}*, K_{99}*, K_{1111}*. The output vector is the maximum deflection (W_{max}*).

Table-5. The input vectors for the linear static response at the Center of a clamped-clamped Beam.

F_1*	w_1*	w_3*	w_5*	w_7*	w_9*	w_{11}*	K_{11}*	K_{33}*	K_{55}*	K_{77}*	K_{99}*	K_{1111}*
0-250	1,58	-1,41	1,41	-1,41	1,41	-1,41	500,6	14,6 10^3	89,1 10^3	30,8 10^4	79,3 10^4	169,1 10^4

The neural network diagram is shown in Figure-11 (a).

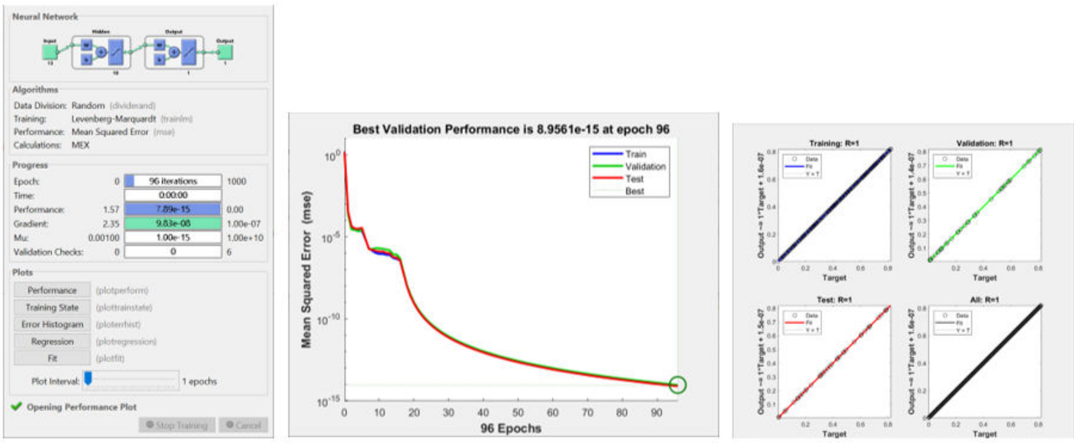

(a) (b) (c)

Figure-11. Schematic Representation of ANNs Architecture, Performance graph, and Regression graph for Rectangular Static linear Response at the Center of Clamped Clamped Beams.

According to Figure-11 (b), the neural network stops at the 15th epoch, and the mean squared error (MSE) at that point is close to 10⁻15. The value of R from the regression analysis is 1, as shown in Figure11(c).

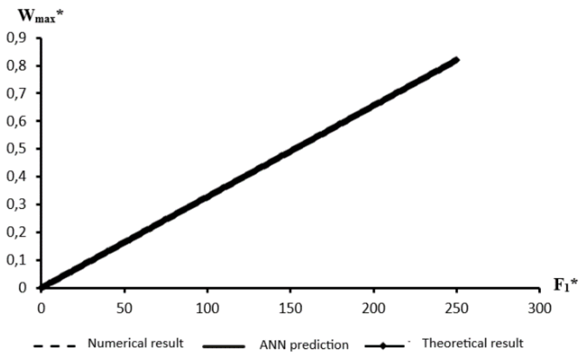

Figure-12. Comparison between the results of ANN prediction, numerical results, and theoretical results (Moulay Abdelali and Benamar, 2024).

3.6 Prediction of the Static Linear Response at One-Quarter and Three-Quarters of a clamped-clamped Beam

For the linear case, the neural network consists of an input layer with 13 input variables, a hidden layer with 10 neurons, and an output layer with a single output variable.

The input vectors for the rectangular beams illustrated in Table-6 are the excitation F_1*, the beam functions: w_1*, w_3*, w_5*, w_7*, w_9*, w_{11}*, and the stiffness values: K_{11}*, K_{33}*, K_{55}*, K_{77}*, K_{99}*, K_{1111}*. The output vector is the maximum deflection (W_{max}*).

ARPN Journal of Engineering and Applied Sciences

Table-6. The input vectors for the linear static response at One-Quarter and Three-Quarters of a clamped-clamped Beam.

F_1*	w_1*	w_3*	w_5*	w_7*	w_9*	w_{11}*	K_{11}*	K_{33}*	K_{55}*	K_{77}*	K_{99}*	K_{1111}*
0-250	0,86	1,44	1,37	0,57	0,53	1,30	500,6	$3,8\ 10^{3}$	$14,6\ 10^{3}$	$39,9\ 10^{3}$	$89,1\ 10^{3}$	$17,4\ 10^{4}$

The neural network diagram is shown in Figure-13 (a).

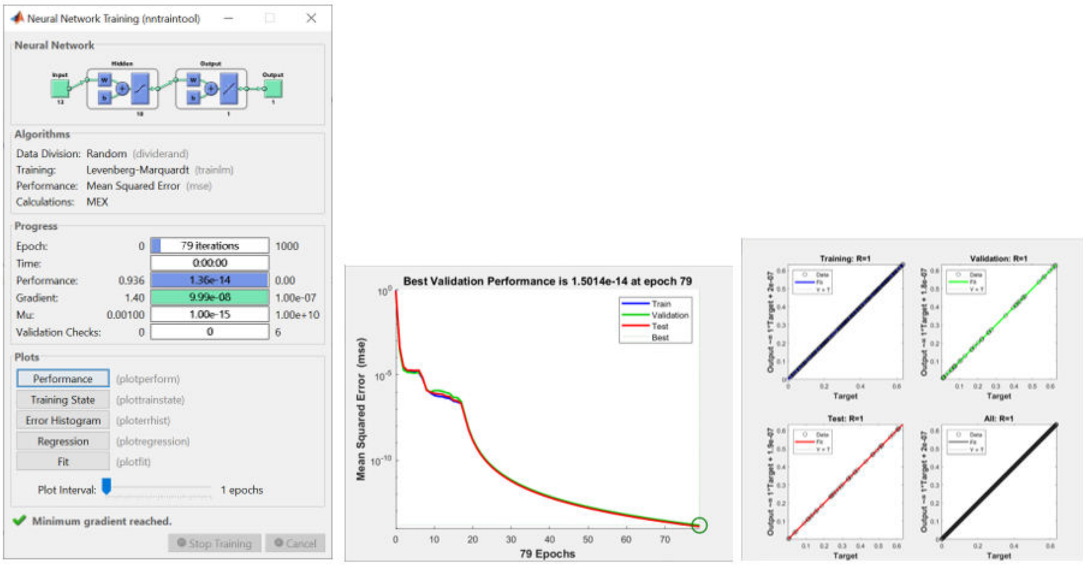

(a) (b) (c)

Figure-13. Schematic Representation of ANNs Architecture, Performance graph, and Regression graph for Rectangular Static linear Response at the One-Quarter and Three-Quarters of clamped-clamped Beams.

According to Figure-13 (b), the neural network stops at the 15th epoch, and the mean squared error (MSE) at that point is close to 10^{-15}. The value of R from the regression analysis is 1, as shown in Figure-13 (c).

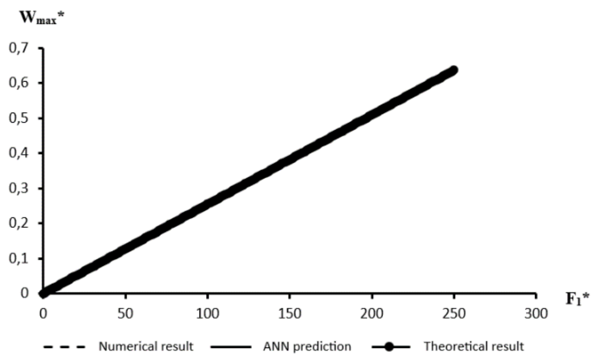

Figure-14. Comparison between the results of ANN prediction, numerical results, and theoretical results (Moulay Abdelali and Benamar, 2024).

3.7 Prediction of the Static Nonlinear Response at the Center of a clamped-clamped Beam

For the nonlinear case, the neural network consists of an input layer with 20 input variables, a hidden layer with 10 neurons, and an output layer with a single output variable.

The input vectors for the rectangular beams illustrated in Table-7 are the excitation F_1*, the contribution coefficient a_1, the beam functions: w_1*, w_3*, w_5*, w_7*, w_9*, w_{11}*, the stiffness values: K_{11}*, K_{33}*, K_{55}*, K_{77}*, K_{99}*, K_{1111}* and the nonlinear stiffness b_{1111}*, b^*_{3111}, b^*_{5111}, b^*_{7111}, b^*_{9111}, b^*_{11111}. The output vector is the maximum deflection (W_{max}*).

Table-7. The input vectors for the nonlinear static response at the Center of a clamped-clamped Beam.

F_1*	a_1	w_1*	w_3*	w_5*	w_7*	w_9*	w_{11}*	K_{11}*	K_{33}*	K_{55}*	K_{77}*
[0-1180]	[0-1]	1,58	-1,40	1,41	-1,41	1,41	-1,41	500,56	14,6 10^3	89,1 10^3	30,8 10^4

K_{99}*	K_{1111}*	b_{1111}*	b^*_{3111}	b^*_{5111}	b^*_{7111}	b^*_{9111}	b^*_{11111}
79,3 10^4	16,9 10^5	12,30	-9,73	-7,61	-6,11	-5,07	-4,28

The neural network diagram is shown in Figure-15 (a).

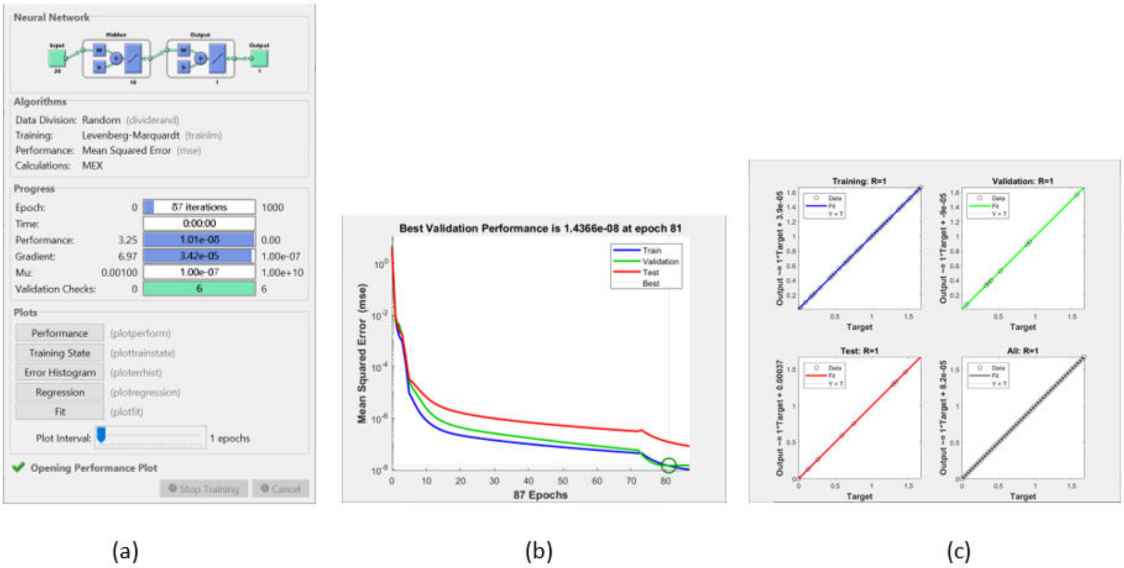

Figure-15. Schematic Representation of ANNs Architecture, Performance graph, and Regression graph for Rectangular Static nonlinear Response at the Center of a clamped-clamped Beam.

According to Figure-15 (b), the neural network stops at the 15th epoch, and the mean squared error (MSE) at that point is close to 10^{-10}. The value of R from the regression analysis is 1, as shown in Figure-15 (c).

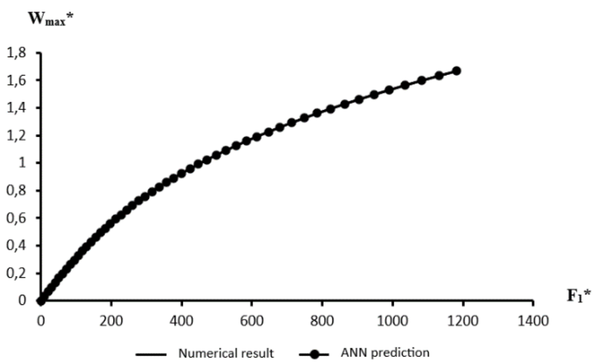

Figure-16. Comparison between the results of ANN prediction and numerical results (Moulay Abdelali and Benamar, 2024).

ISSN 1819-6608
ARPN Journal of Engineering and Applied Sciences

3.8 Prediction of the Static Nonlinear Response at One-Quarter and Three-Quarters of a clamped-clamped Beam

For the nonlinear case, the neural network consists of an input layer with 19 input variables, a hidden layer with 10 neurons, and an output layer with a single output variable.

The input vectors for the rectangular beams illustrated in Table-8 are the excitation F_1*, the contribution coefficient a_1, the beam functions: w_1*, w_2*, w_3*, w_4*, w_5*, w_6*, the stiffness values: K_{11}*, K_{22}*, K_{33}*, K_{44}*, K_{55}*, K_{66}* and the nonlinear stiffness b_{1111}*, b^*_{2111}, b^*_{3111}, b^*_{5111}, b^*_{6111}. The output vector is the maximum deflection (W_{max}*).

Table-8. The input vectors for the nonlinear static response at One-Quarter and Three-Quarters of a clamped-clamped Beam.

F_1*	a_1	w_1*	W_2*	W_3*	W_4*	W_5*	W_6*	K_{11}*	K_{22}*	K_{33}*	K_{44}*
0-1180	0-1	0,86	1,44	1,37	0,57	0,53	1,30	500,56	3,8 10^3	14,6 10^3	39,9 10^3

K_{55}*	K_{66}*	b^*_{1111}	b^*_{3111}	b^*_{5111}
89,1 10^3	17,4 10^4	12,30	-9,73	-7,61

The neural network diagram is shown in Figure-17(a).

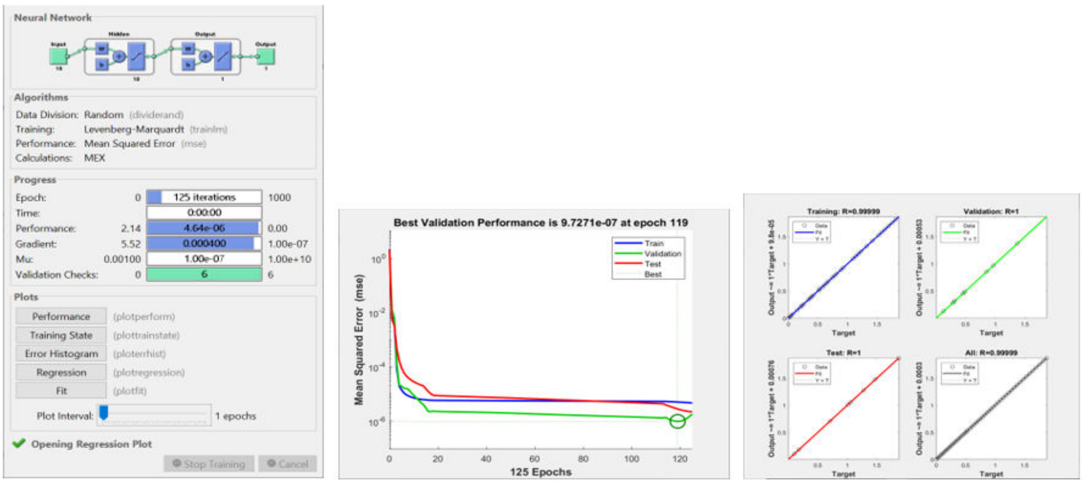

(a) (b) (c)

Figure-17. Schematic Representation of ANNs Architecture, Performance graph, and Regression graph for Rectangular Static nonlinear Response at the One-Quarter and Three-Quarters of a clamped-clamped Beam.

According to Figure-17 (b), the neural network stops at the 15th epoch, and the mean squared error (MSE) at that point is close to 10^{-10}. The value of R from the regression analysis is 1, as shown in Figure-17 (c).

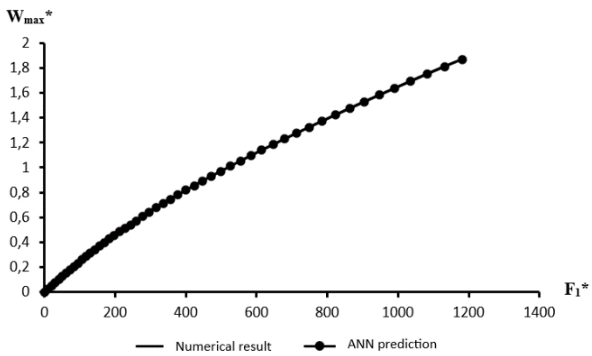

Figure-18. Comparison between the results of ANN prediction and numerical results (Moulay Abdelali and Benamar, 2024).

ARPN Journal of Engineering and Applied Sciences

Figures 19 and 20 show the maximum dimensionless values of the transverse displacement for both a simply supported beam and a clamped beam subjected to a concentrated dimensionless force applied at the midpoint, as well as at the one-quarter and three-quarter points along the span. The curve indicates that the transverse displacement values are greater for the simply supported beam compared to the clamped-clamped beam, which is consistent with theoretical results.

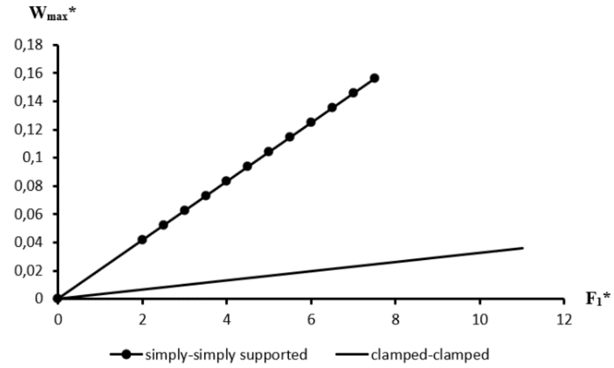

Figure-19. Comparison of the maximum linear displacement at the center of a simply supported beam on both sides and a clamped-clamped beam.

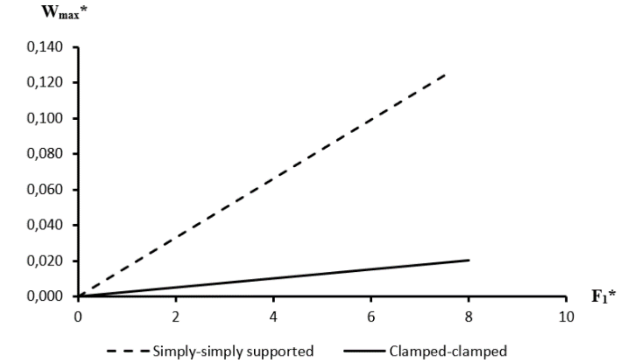

Figure-20. Comparison of the maximum linear displacement at the One-Quarter and Three-Quarters of a simply supported beam on both sides and a clamped-clamped beam.

Figures 21 and 22 depict the nonlinear dimensionless values of the transverse displacement for a simply supported beam and a clamped beam subjected to a concentrated dimensionless force applied at the midpoint, as well as at the one-quarter and three-quarter points along the span. The nonlinear curve shows a hardening behavior, with the displacement increasing nonlinearly as the applied force on the beam increases. These results align with expectations, as nonlinearity typically stiffens the beam, leading to a nonlinear response. The curve also indicates that for the same range of applied force, transverse displacement values are greater for the simply supported beam compared to the clamped-clamped beam.

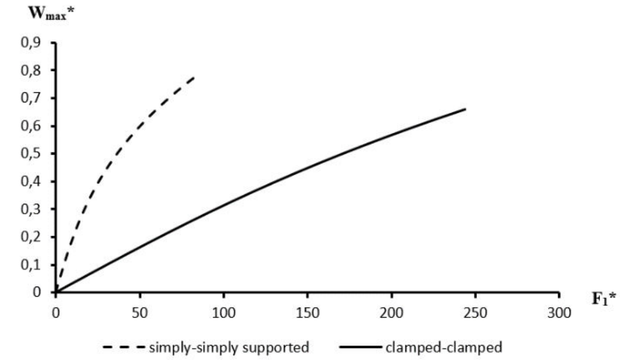

Figure-21. Comparison of the maximum nonlinear displacement at the center of a simply supported beam on both sides and a clamped-clamped beam.

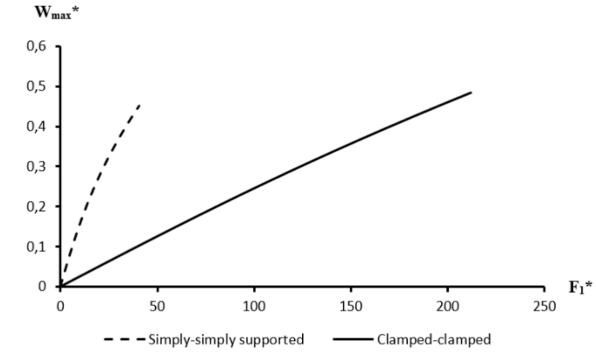

Figure-22. Comparison of the maximum nonlinear displacement at the One-Quarter and Three-Quarters of a simply supported beam on both sides and a clamped-clamped beam.

4. CONCLUSIONS

The prediction of the static linear and nonlinear response of simply supported and cantilever beams excited by different concentrated forces at the center, one-quarter, and three-quarters was developed by training several neural networks. The validation of the results was confirmed by comparing them with numerical results based on the Rayleigh-Ritz method, theoretical calculations, and findings in the literature. The Levenberg-Marquardt algorithm produced very good results with fewer iterations and improved accuracy. The maximum displacement increases parabolically with the excitation value. The maximum linear and nonlinear displacements of the simply supported and cantilever beams were compared at the center, one-quarter, and three-quarters.

REFERENCES

Murali Krishna B., Guru Prathap Reddy V., Shafee M., Tadepalli T. 2020. Condition assessment of RC beams using artificial neural networks. Structures 23, 1-12. https://doi.org/10.1016/j.istruc.2019.09.014

Song Y., Yu Z. June 2013. Springback prediction in T-section beam bending process using neural networks and finite element method. Archives of Civil and Mechanical Engineering, 13(2): 229-241. DOI:10.1016/j.acme.2012.11.004

Sakr A., Sakla S. S. 2009. Long-term deflection of cracked composite beams with nonlinear partial shear interaction - A study using neural networks, Engineering Structures 31, 2988-2997.
https://doi.org/10.1016/j.engstruct.2009.07.027

Hosseini M., Abbas H. 2012. Neural network approach for prediction of the deflection of clamped beams struck by a mass, Thin-Walled Structures, 60, 222-228. https://doi.org/10.1016/j.tws.2012.06.006

Nguyen H. D., Zhang Q., Choi E., Duan W. 2020. An improved deflection model for FRP RC beams using an artificial intelligence-based approach. Engineering Structures, 219: 110793.
DOI: 10.1016/j.engstruct.2020.110793

Hasançebi O., Dumlupınar T. 2013. Linear and nonlinear model updating of reinforced concrete T-beam bridges using artificial neural networks. Computers and Structures, 119, 1-11.
https://doi.org/10.1016/j.compstruc.2012.12.017

Tadesse Z., Patel K. A., Chaudhary S., Nagpal A. K. 2012. Neural networks for prediction of deflection in composite bridges. Journal of Constructional Steel Research, 68, 138-149. https://doi.org/10.1016/j.jcsr.2011.08.003

Moulay Abdelali H., Benamar R. 2024. Non-linear static behavior of simply supported and clamped-clamped beams subjected to a concentrated load. Materials Today: Proceedings, 14.
https://doi.org/10.1016/j.matpr.2024.02.016

Abolfathi A., Waters T. P., Brennan M. J. 2010. Large deflection of a simply supported beam. ISVR Technical Memorandum No. 988, University of Southampton Institute of Sound and Vibration Research Dynamics Group, research gate, August.